Title
Implementing Mass Cytometry at the Bedside to Study the Immunological Basis of Human Diseases: Distinctive Immune Features in Patients with a History of Term or Preterm Birth.

Permalink
https://escholarship.org/uc/item/0c4566zh

Journal
Cytometry Part A, 87(9)

Authors
Gaudillière, Brice
Ganio, Edward
Tingle, Martha
et al.

Publication Date
2015-09-01

DOI
10.1002/cyto.a.22720

Peer reviewed

Implementing Mass Cytometry at the Bedside to Study the Immunological Basis of Human Diseases: Distinctive Immune Features in Patients with a History of Term or Preterm Birth

Brice Gaudillière[1,2], Edward A. Ganio[1], Martha Tingle[1], Hope L. Lancero[1], Gabriela K. Fragiadakis[2,3], Quentin J. Baca[1], Nima Aghaeepour[2], Ronald J. Wong[4], Cele Quaintance[4], Yasser Y. El-Sayed[5], Gary M. Shaw[4], David B. Lewis[4], David K. Stevenson[4], Garry P. Nolan[2,3], and Martin S. Angst[1,*]

[1]Department of Anesthesiology, Perioperative, and Pain Medicine, Stanford University, School of Medicine, Stanford, California 94305

[2]Baxter Laboratory in Stem Cell Biology, Department of Microbiology and Immunology, Stanford University, Stanford, California 94305

[3]Department of Microbiology and Immunology, Stanford University, Stanford, California 94305

[4]Department of Pediatrics, Stanford University School of Medicine, Stanford, California 94305

[5]Department of Obstetrics and Gynecology, Stanford University School of Medicine, Stanford, California 94305

Abstract

Single-cell technologies have immense potential to shed light on molecular and biological processes that drive human diseases. Mass cytometry (or Cytometry by Time Of Flight mass spectrometry, CyTOF) has already been employed in clinical studies to comprehensively survey patients' circulating immune system. As interest in the "bedside" application of mass cytometry is growing, the delineation of relevant methodological issues is called for. This report uses a newly generated dataset to discuss important methodological considerations when mass cytometry is implemented in a clinical study. Specifically, the use of whole blood samples versus peripheral blood mononuclear cells (PBMCs), design of mass-tagged antibody panels, technical and analytical implications of sample barcoding, and application of traditional and unsupervised approaches to analyze high-dimensional mass cytometry datasets are discussed. A mass cytometry assay was implemented in a cross-sectional study of 19 women with a history of term or preterm birth to determine whether immune traits in peripheral blood differentiate the two groups in the absence of pregnancy. Twenty-seven phenotypic and 11 intracellular markers were simultaneously analyzed in whole blood samples stimulated with lipopolysaccharide (LPS at 0, 0.1, 1, 10, and 100 ng mL^{-1}) to examine dose-dependent signaling responses within the toll-like receptor 4 (TLR4)

---

[*]Correspondence to: Martin S. Angst, Department of Anesthesia, Office S276, Grant Building, 300 Pasteur Drive, Stanford, CA 94305-5117. ang@stanford.edu.

pathway. Complementary analyses, grounded in traditional or unsupervised gating strategies of immune cell subsets, indicated that the prpS6 and pMAPKAPK2 responses in classical monocytes are accentuated in women with a history of preterm birth (FDR<1%). The results suggest that women predisposed to preterm birth may be prone to mount an exacerbated TLR4 response during the course of pregnancy. This important hypothesis-generating finding points to the power of single-cell mass cytometry to detect biologically important differences in a relatively small patient cohort.

Key terms

mass cytometry; CyTOF; clinical applications; innate immunity; single cell; preterm birth; monocytes; TLR4

The recent expansion of single-cell technologies has triggered significant interest in leveraging the power of high-content single-cell analysis for use in clinical studies. Among these technologies, mass cytometry, which currently allows for the simultaneous measurement of over 50 parameters per single cell (1,2), has been successfully implemented at the bedside to comprehensively survey the circulating immune system in patient blood samples (3). For example, in a study of patients undergoing surgery, mass cytometry revealed immune signatures of surgical trauma that contained strong correlates of clinical recovery in a subset of monocytes (4). Thus, the application of this multiplexed, high-content, and comprehensive single-cell assay to clinical samples has enormous potential to illuminate the immunological basis of human disease processes (5).

With the rapid adoption of mass cytometry by an ever-growing user population, significant effort has been devoted to standardizing mass cytometry in practice (6–9). However, several key methodological issues remain that need to be carefully delineated when employing mass cytometry in clinical studies. These include the use of whole blood versus peripheral blood mononuclear cells (PBMCs), the design of the antibody panel, the use of external ligands and ligand concentrations to evoke functional responses in immune cell subsets, the intricacies of mass cytometry (such as barcoding and normalization procedures), and the application of traditional and non-traditional analytical approaches to maximize knowledge gained from the high-dimensional datasets. This report uses a set of mass cytometry and clinical data to discuss and illustrate these important considerations.

Data were collected in this study from non-pregnant women with a history of term or preterm birth. Preterm birth affects 5–13% of pregnancies in developed countries and is the leading cause of neonatal deaths (10,11). Two-thirds of preterm births occur after the spontaneous onset of labor, which is associated with a switch from an anti- to a pro-inflammatory state (12). Innate immune cells play a critical role in regulating these inflammatory processes (13). Some of their relevant functional attributes are reflected in peripheral blood in pregnant women. For example, differences in lipo-polysaccharide (LPS)-evoked release of IL-10 in PBMCs have been linked to term and preterm births (14). The primary aim of this study was to determine whether immune traits in peripheral blood in the absence of pregnancy could differentiate between women with a history of term or preterm birth.

Methods

Clinical Design

Patient population—The study was approved by the Institutional Review Board of Stanford University School of Medicine (Stanford, CA). Subjects were recruited through either: (1) radio, newspaper, and targeted mail advertisements or (2) at the Stanford Clinics. Inclusion criteria were: (1) age 18–45 years and (2) history of term (>37 gestational wks) or pre-term birth (>27 and <35 gestational weeks). An additional inclusion criterion for women with a history of preterm birth was the preterm birth had to be spontaneous. The rational for choosing a preterm time period of 27–34 weeks was to increase the homogeneity of the preterm study group by excluding women with a history of very early preterm birth and by creating a minimal difference in gestational weeks at birth between the two study groups of 3 weeks. Exclusion criteria for women of both groups were: (1) last delivery <6 months, (2) breastfeeding, (3) plans to become pregnant, (4) irregular hormonal cycle, (5) metabolic or autoimmune disease, (6) current infectious disease (ongoing fever, cough or rash, current antibiotic treatment, or history of chronic bacterial or viral infections such as HIV or hepatitis), (7) clinically relevant cardiovascular, pulmonary, renal, or hepatic disease, (8) medications with possible immune-modulating effects (e.g., teroids), (9) smoking, and (10) history of alcohol or drug abuse. Additional exclusion criteria included previous preterm birth due: to (1) multiple gestation, (2) polyhydramnios, (3) placenta previa or abruption, (4) fever at birth, and (5) stated diagnosis of chorioamnionitis.

Sample collection—Participants were screened for inclusion and exclusion criteria by phone. They were required to abstain from alcohol and caffeine for >12 h, get at least 6 h of nighttime sleep, and abstain from eating and drinking for >6 h before their study visit. The study visit took place between menstrual cycle days 1–7. Written informed consent was obtained before confirming participants' medical and medication history as well as their demographic information. A single venous blood draw (30 mL) was collected into heparinized tubes (sodium heparin, BD Biosciences, San Jose, CA) between 7 and 9 AM and immediately delivered to the laboratory for further processing.

Mass Cytometry-specific Experimental Design

An overview illustrating sample collection, sample processing, and data analyses is provided in Figure 1. Individual steps are discussed below.

Assaying whole blood

__General considerations:__ The assay was performed in whole blood samples kept at room temperature rather than in PBMCs to minimize sample processing steps and preserve immune cells in as close to in vivo conditions as possible. Importantly, samples were stimulated with external ligands (if applicable), fixed, and stored at −80°C within 60 min of whole blood collection.

There are several important differences between assaying whole blood or PBMCs. Cells in whole blood are fixed within 60 min of collection, while PBMCs are frozen in liquid nitrogen as live cells. Because cells in whole blood are fixed before being stored, stimulation

of these cells with external ligands has to occur before storage. In contrast, PBMCs are stimulated after samples are removed from storage and thawed. However, fixing and storing immune cells directly in whole blood samples has the advantage of preserving all immune cell populations (including granulocytes) and avoiding a density gradient centrifugation step common in PBMC preparations, which may alter immune cell distribution, cell-surface antigen expression, transcriptional activity (15–19), and introduce potential elemental contaminants (e.g. iodine, barium and other) (20).

Stimulation with external ligands to evoke cellular responses

General considerations: Stimulation of whole blood samples with external ligands occurs within 30 min of sample collection. The choice of ligand(s) is based on the biological question under investigation. In essence, ligands are chosen to perturb signaling pathways in cell subsets that are implicated in disease-related and pathophysiologically important processes in order to unmask disease-specific cellular alterations that may not be detectable in non-perturbed cells (21).

Typically, supra-physiological ligand concentrations are used to evoke the maximum response, thereby testing a cell's functional capacity (1,21). However, stimulation with physiologically more relevant concentrations may reveal biologically important differences in cellular responses that are independent of their functional capacity. The importance of mimicking physiological conditions was highlighted in a recent article by Kay et al. demonstrating that polyfunctionality in natural killer (NK) and T cells to the pH1N1 virus was increased during pregnancy, while responses to the non-physiological ligands phorbol 12-myristate 13-acetate and ionomycin were reduced (22). In the current study, the exploration of ligand concentration versus response functions allowed for a more comprehensive characterization of cellular functions.

Specific protocol: In this study, LPS was chosen as it selectively binds to the toll-like receptor 4 (TLR4). TLR4 signaling plays an important role in the maintenance of pregnancy (23,24). More specifically, in mice, intrauterine infusion of LPS reproducibly induces preterm birth, a phenomenon that depends on the presence of a functional TLR4 receptor (25). Furthermore, in a longitudinal study of women during pregnancy, Harper et al. found that the LPS-induced production of IL-10 in PBMCs correctly stratified women into preterm and term birth groups (14).

To examine potential differences in signaling responses to LPS, each patient sample was stimulated with five concentrations of LPS (0, 0.1, 1, 10, and 100 ng mL^{-1}) for 15 min at 37°C. Blood samples (1 mL) were re-suspended in 1.4 mL stabilizing buffer (Smart Tube, Palo Alto, CA), incubated for 10 min at room temperature for fixation, cooled to 4°C, and stored at −80°C for further processing. Experiments in independent samples (results not shown) established that the highest concentration included in this protocol evoked the maximum signaling response.

Metal-conjugated antibody panel design and validation

General considerations: Currently, mass cytometry allows for the simultaneous detection of 50 metal isotopes (rare earth elements). Each metal is conjugated to a unique antibody that recognizes either an extracellular epitope (typically for identification of immune cell subsets) or an intracellular epitope (for example a phospho-epitope specific to the activated form of a signaling protein). Using 50 metal-conjugated antibodies simultaneously affords the detailed phenotypical characterization of immune cell subsets and the concomitant exploration of multiple cell signaling pathways.

The composition of the antibody panel is guided by the particular biological question, antibody availability and specificity, and mass cytometry related specifications. Each antibody must be validated by titration to establish sufficient sensitivity and specificity in cell populations known to either stain positive or negative. In addition, several machine and isotope-specific considerations have to be taken into account when pairing an antibody with its metal conjugate. These include isotopic impurity and machine-specific abundance sensitivity, i.e., the ratio between the signal observed at the $M \pm 1$ mass channels (neighboring channels) and the signal at the M channel (estimated at <2%) as well as the propensity of some metal ions to form strong oxides producing a contaminating signal in the $M + 16$ channel. For example, the metal conjugates La, Ce, Pr, and Nd are known to oxidize more readily than other metal isotopes, producing ~2–3% $M + 16$ oxidation signals. Therefore, antibodies against phospho-specific epitopes, which are typically associated with a smaller signal than antibodies directed against more abundant phenotypical markers, are usually conjugated to metals that do not overlap with the $M + 16$ position of La, Ce, Pr, or Nd. Machine-specific abundance sensitivity matrices are publically available and are useful guides when designing antibody panels for mass cytometry (www.fluidigm.com). Another important consideration includes metal-specific sensitivity patterns. As Tricot et al. recently quantified, lanthanides are detected with different sensitivities as a function of their atomic mass (26). Metals with atomic masses in the mid-range of the detector (atomic masses 159–169) are detected more efficiently. As such, to improve the detection of low-abundance antigens (e.g., certain phosphorylated epitopes), antibodies against such antigens are typically conjugated to metals with masses in the mid-range of the detector.

Specific protocol: In this study, antibodies against 27 phenotypic markers were chosen to characterize major immune cell types previously implicated in the pathophysiology of feto-maternal tolerance and maintenance of pregnancy (Supporting Information Table 1) (12,23,24). Gating of immune cells using these antibodies identified granulocytes, classical (cMC) and non-classical monocytes (ncMC), NK cells, B cells, myeloid dendritic cells (DCs), CD4^{+} and CD8^{+} T cells (naive, memory), regulatory T cells (T_{regs}), $\gamma\delta$T cells, and their subsets (Supporting Information Figs. 1 and 2).

Seven antibodies against functional markers were selected to interrogate canonical components of the TLR4 pathway, including pP38, pPERK, pMAPKAPK2, prpS6, pCREB, IκB, and pNFκB. The panel also included four additional antibodies targeting STAT 1, 3, 5, and 6 to examine responses to the alternative external ligands IFNα, IL-2, IL-4, IL-6, and GM-CSF. While these ligands were not included in the current study, they are used in

ongoing longitudinal studies of pregnant women as the pathways examined may be affected by pregnancy (27).

All antibodies were tested for specificity and sensitivity across a range of concentrations (typically, 0.25–4 μg mL^{-1}) as described in Gaudilliere et al. (4). All but two antibodies (CCR6 and CXCR3) produced antigen-specific staining. Antibodies against CCR6 and CXCR3 were thus omitted from the panel. A subset of the antibodies was obtained pre-labeled from Fluidigm (Fluidigm, South San Francisco, CA), while others were metal-labeled as described by Bendall et al. (1). In designing the antibody panel, considerations were given to isotopic purity and oxidation propensity. Qualitative knowledge of metal sensitivity patterns across the detector's mass range was utilized to conjugate metals detected with higher sensitivity to antibodies recognizing low-abundance antigens, however quantitative data was not available at the time of the study.

Antibodies were obtained in carrier-protein-free PBS and labeled using the MaxPAR antibody conjugation kit (Fluidigm) according to the manufacturer's protocol. All metal-labeled antibodies were diluted based on their percent yield by measurement of absorbance at 280 nm to 0.2 mg mL^{-1} in Candor PBS Antibody Stabilization solution (Candor Biosciences, Wangen, Germany) for storage at 4°C. Cells were washed once with cell staining media (CSM, phosphate buffered saline with 0.5% bovine serum albumin, 0.02% NaN$_3$) and then incubated for 10 min at room temperature with one test of FcX block (Biolegend, San Diego, CA) to block non-specific Fc binding. Cells were stained with all surface antibodies for 30 min and washed once with CSM. Cells were permeabilized with 1 mL of methanol for 10 min on ice. Cells were then washed twice with PBS and once with CSM and incubated with the intracellular antibody cocktail for 30 min at room temperature. Cells were washed once with CSM then incubated overnight at 4°C with an iridium-containing intercalator (Fluidigm) in PBS with 1.6% formaldehyde. Cells were then washed twice with CSM, once with water, and resuspended in a solution of normalization beads as previously described (8). Cells were filtered through a 35-μm membrane prior to analysis by mass cytometry.

Barcoding

__General considerations:__ Mass-tag barcoding of patient samples minimizes experimental variability caused by antibody staining of different samples or changes in instrument sensitivity when assaying different samples (28,29). Bar-coding also reduces time requirements for analyzing samples with mass cytometry. Using unique combinations of three out of six palladium (Pd) isotopes enables the simultaneous staining and analysis of 20 different patient samples (as there are 20 possible isotope combinations). It also provides a means to eliminate cell doublets from the analysis as doublets are flagged by more than three Pd-isotopes. However, if >20 samples are analyzed for a given study it is important to consider that the experimental variability between samples of the same barcoded batch is smaller than the variability between samples of different barcoded batches. Samples assigned to the same barcoded batch are those that investigators wish to compare with greatest precision. For example, longitudinal samples obtained in a given patient before and after an intervention should be assigned to the same barcoded batch to infer the effect of an

intervention with greatest precision. Alternatively, single samples of two different patient populations stimulated with various concentrations of external ligands may be best assigned in batches that are grouped by ligand concentrations to infer any group differences for a given ligand concentration.

Specific protocol: The number of patients in this study ($n = 19$) allowed barcoding and simultaneous analysis of all patient samples for a given concentration of LPS (i.e., five barcoded batches or plates for five different concentrations of LPS). This sample barcoding scheme emphasized the minimization of experimental errors between patient samples at a given concentration of LPS rather than between stimulation conditions within a given patient, thus minimizing experimental sources of increased between-patient variability.

Isothiocyanobenzyl-EDTA/Pd (Pd)-based reagents for mass tag barcoding were prepared as described by Zunder et al. (29). Each well of a barcoding plate contained a distinct combination of three Pd isotopes (Pd 102, 104,105, 106, 108, and 110) at 200 nM in DMSO. After thawing and lysing red blood cell in a hypotonic buffer, cells were transferred into a deep-well block and washed once with CSM, once with PBS, and once with 0.02% saponin in PBS. The barcoding plate was thawed, and each well of barcode reagent was diluted in 1 mL 0.02% saponin in PBS. Diluted barcode reagent was transferred to cells, and samples were incubated at room temperature for 15 min, washed twice with CSM, and then pooled for staining.

Mass cytometry

General considerations: The ion detection sensitivity of a mass cytometer drifts during instrument use and can change with weekly maintenance work including cleaning and calibration. As a result the signal intensity for a given isotope can vary irrespective of the actual number of metal ions present in a cell. To compensate for temporal changes in detector sensitivity, mass cytometry results are normalized to the read out of standard beads that are added to all barcoded samples (8).

Specific protocol: Barcoded and antibody-stained cells were analyzed on a CyTOF version 1 mass cytometer instrument equipped with CyTOF software version 5.1.648 (CyTOF 1, Fluidigm) at an event rate of 400–500 cells per sec. The data were normalized using Normalizer v0.1 MCR (8). Files were de-barcoded using a single-cell Matlab Debarcoder Tool (29).

Data analysis

General considerations

Identification of immune cell subsets and quantification of associated signaling responses: Data analysis followed two complementary approaches. The first approach used prior knowledge to phenotype immune cells with canonical cell surface markers and a manual gating strategy (30), and assign functional attributes (e.g., cell signaling events) to identified cell subsets (Supporting Information Fig. 1). In this study LPS-induced modulation of seven signaling proteins (pP38, pERK1/2, pMAPKAPK2, prpS6, pCREB,

pNFκB, and IκB) was inferred for 12 immune cell subsets, four of them known to respond to LPS (granulocytes, classical and non-classical monocytes, and myeloid DCs) (31).

The second approach applied an unsupervised clustering algorithm to define a hierarchy of phenotypically-related cell clusters (Fig. 2). This approach is agnostic and leverages the high parametrization afforded by mass cytometry by utilizing information contained in the expression level of all phenotypic markers measured per single cell. The number of clusters was defined by considering only clusters that contained a minimum of 1% of the total cell number. Functional attributes were then assigned to each cell clusters. The algorithm used for this analysis is contained in the CITRUS package (32).

Several unsupervised clustering algorithms have been developed to automate the gating of immune cells. The performance of these methods was extensively evaluated in the FlowCAP challenge (Flow Cytometry: Critical Assessment of Population Identification Methods) (33). A head-to-head comparison of algorithms included in the FlowCAP-II challenge demonstrated superiority of the CITRUS package with respect to clustering sensitivity measures, the identification of cell subsets with clinical prognostic value, and the capacity to correctly classify patient samples based on their disease states (32).

Choice of statistical packages for identification of immune features associated with a clinical outcome: The manual-gating described above is a model-based approach that is focused by limiting the number of comparisons, is well suited for examining hypothesis-driven questions, and justifies the use of stringent statistical tests including traditional Bonferroni correction for multiple comparisons to detect significant differences between groups.

By contrast, the unsupervised clustering of immune cell subsets is more explorative and hypothesis-generating. This approach produces a large data matrix and a vast number of comparisons as immune features compared between groups include cell frequency within each cluster as well as all cluster-specific functional attributes. In such high-dimensional data-sets, the use of traditional statistical approaches including Bonferroni correction is considered too stringent as biologically important differences may be missed. This has led to the development of alternative approaches, most notably the significance analysis of microarrays (SAM) (34). SAM is a non-parametric test specifically designed for calculating robust false discovery rates of high-dimensional datasets by artificially introducing a large number of permutations (bootstraps). This approach is generally less stringent than adjustment for multiple comparisons using Bonferroni's method.

Other statistical methods adapted to the analysis of high-dimensional mass cytometry datasets use regularized supervised learning algorithms to identify stratifying immune features that best predict clinical outcomes. For example, CITRUS constructs classification models using the lasso regularized logistic regression and nearest shrunken centroid methods (35). After cross-validation, the investigator identifies models having a low or acceptable error rate. In comparison to SAM, regularized learning algorithms assess the predictive value of a given model. As the primary goal of the current study was hypothesis-generating

in nature, these statistically more predictive methods requiring larger patient cohorts were not applicable.

Specific protocol: Manual gating of 12 distinct immune cell types was performed in nolanlab.cytobank.org using the Cytobank online platform (Cytobank, Inc., Mountain View, CA) as previously described (4). Ligand concentration-dependent LPS-induced modulation of the seven signaling proteins pP38, pERK1/2, pMAPKAPK2, prpS6, pCREB, pNFκB, and IκB were inferred for all immune cell subsets (5 ligand concentrations, 7 signaling proteins, 12 cell types) and compared between studied groups (Bonferroni-adjusted $P = 0.00012$). Statistical analysis was performed using SPSS version 20 (IBM SPSS Statistics) and graphical representation was performed using GraphPad Prism version 6.0d (GraphPad Software).

The hierarchical clustering approach (Ward's linkage and Euclidean distance in R) used the CITRUS analytical package for the detailed characterization and visual representation of CD45$^+$CD66$^-$ cells (32). Ten thousand events were sampled from each patient sample. The cluster hierarchy plots and histograms were created in R. For each cluster (157), cell frequency (as a percent of total CD45$^+$CD66$^-$) and the median signal intensity of each functional marker (7) were determined for each LPS concentration (5) resulting in 5495 parameters. Statistical significance was inferred with the "samr" package SAM 2-class unpaired using a false discovery rate of 1%. For the biaxial representation of CITRUS clusters, FCS files generated from cells contained within indicated clusters or groups of clusters were imported into and visualized using Cytobank.

Results

Subjects

Four hundred subjects were screened in total. One hundred and two met inclusion criteria for preterm birth. Of those, 64 did not pass exclusion criteria and 29 refused to participate. The final analysis included complete datasets from 19 women, 9 women with a history of preterm birth (preterm group, 6 Caucasian and 3 Asian) and 10 women with a history of term birth (term group, 5 Caucasian and 5 Asian). In the preterm and term groups, the median ages were: 39 years (IQR 35–43) and 42 years (IQR 38–43), the median body mass indices (BMI) were: 26 kg m^{-2} (IQR 21–33) and 24 kg m^{-2} (IQR 20–30), the median numbers of pregnancies were: 2 (range 2–3) and 2 (range 1–4), and the average times since the last delivery were: 4.6 years (IQR 2–6.5) and 4.5 years (IQR 2–7). No statistically significant differences were detected between groups (Mann–Whitney U test, $P > 0.05$). The median gestational age at delivery was 31 week (range 24–34) in the preterm group and 39 weeks (range 38–40) in the term group. Comorbidities included asymptomatic benign cardiac arrhythmia ($n = 2$), mild eczema ($n = 2$), mild and well-controlled asthma ($n = 2$), and depression ($n = 2$). Of the nine women with a history of preterm birth one had one preterm birth, three had two preterm births, two had three preterm births, one had four preterm births, one had one pre-term and one term birth, and one had two preterm and two term births.

Immune Cell Distribution in Non-pregnant Women with a History of Preterm or Term Birth

Manual gating identified granulocytes, classical and non-classical monocytes, NK cells, myeloid DCs, CD4$^+$ and CD8$^+$ T cells (naive, memory), T$_{regs}$, $\gamma\delta$T cells, and B cells (Supporting Information Fig. 1). Cell frequencies were expressed as percent total immune cells for granulocytes, and percent CD45$^+$CD66$^-$ mononuclear cells (Fig. 3). No statistical differences in cell frequencies were detected between the preterm and term groups (Mann–Whitney U test, Bonferroni adjusted P values = 0.004). To identify differences in cell frequencies that may have been overlooked by manual gating, the analysis was expanded to the 157 cell clusters identified by unsupervised clustering (32) (Fig. 2). No significant differences were detected between the study groups. Results indicated that in the non-pregnant state, women with a history of preterm or term birth share a similar distribution pattern of immune cell subsets.

Stimulation with LPS Evokes Dose-dependent and Cell-type-specific Signaling Responses

Stimulation with LPS induced the dose-dependent phosphorylation of P38, ERK1/2, MAPKAPK2, rpS6, CREB, NFκB and the concomitant degradation of IκB in a subset of manually gated cell types in samples from both study groups (Figs. 4 and 5). Consistent with established cell-type specificity for LPS-mediated TLR4 signaling, robust signaling responses to maximal LPS concentration were only detected in granulocytes, classical and non-classical monocytes, and myeloid DCs, but not in other examined cell types (Fig. 4). In monocytes and dendritic cells even the lowest LPS concentration (0.1 ng mL^{-1}) induced highly significant signaling responses for rpS6 and IκB (Fig. 5, P values $<10^{-5}$).

Remarkably, signaling responses across the 420 examined conditions (5 concentrations, 12 cell types, 7 functional markers) were tightly distributed around median signal intensities with a median coefficient of variation of 12% in the term group (IQR [7.9%, 22%]) and 13% in the preterm group (IQR [8.6%, 23%]). This highlights the capacity of a mass cytometry-based assay to precisely quantify functional immune responses across many cell types in a relevant patient population.

Having established a precise and cell-type-specific assay, the first analytical approach focused on signaling responses in manually gated granulocytes, classical and non-classical monocytes, and myeloid DCs (Fig. 5, Supporting Information Table 2). LPS induced more pronounced prpS6, pERK, and pMAPKAPK2 signals in monocytes and DCs of women with a history of preterm rather than term births (Supporting Information Table 2, Figs. 5A–5C). However, these results did not reach statistical significance after Bonferroni correction.

Signaling Responses to LPS in Classical Monocytes Identify Patients with a History of Preterm Birth

To investigate differences between the two study groups that may have gone undetected using the first model-based and statistically more stringent approach, the CITRUS analytical package was applied to interrogate all signaling responses to LPS across a hierarchy of immune cell clusters spanning the entire immune system. Six immune features differentiating the two study groups were identified (Fig. 6). Consistent with results from manually gated cells, the prpS6 and pMAPKAPK2 responses to LPS (0.1 ng mL^{-1}) in a

classical monocyte cluster were more pronounced in the preterm group. SAM also identified the pMAPKAPK2 signal in two B-cell clusters and a naive CD4^{+} T-cell cluster, and the pERK1/2 signal in a memory CD4^{+} T-cell cluster. Because LPS induced little phosphorylation of MAPKAPK2 in B cells or CD4^{+} T cells, and ERK1/2 in CD4^{+} T cells across the range of the tested concentration (Fig. 4), the biological relevance of these additional features warrants further investigation.

Results from the hierarchical clustering approach with CITRUS suggest that in the absence of pregnancy, the majority of immune cells from women with a history of preterm or term birth respond similarly to an LPS challenge. However, statistically significant (FDR <1%) differences between the two study groups were detected for signaling responses in classical monocytes to low LPS concentrations. This corroborates results of the manual gating approach (Supporting Information Table 2; $P = 0.002–0.044$).

Discussion

Implementing mass cytometry in clinical studies in order to examine immunological aspects of particular disease processes has recently received significant scholarly attention (5). However, the successful execution of a mass-cytometry-based clinical study requires the assembly of novel methodologies and analytical tools, which have not yet been clearly delineated. Here, we present the results of a study examining immune signatures that may differentiate women with a history of term birth from those with a history of preterm birth in order to illustrate the important methodological issues that should be considered when mass cytometry is implemented at the bedside and when the resulting high-dimensional dataset is linked to a given clinical outcome. We also present evidence suggesting that LPS-evoked signaling responses in classical monocytes may be more pronounced in non-pregnant women with a history of preterm birth. This is an important hypothesis-generating finding that points to the power of single-cell mass cytometry to detect biologically important differences in a relatively small patient cohort.

Important considerations in the design of a clinical study employing mass cytometry include: (i) logistical requirements to ensure seamless and timely collection of clinical samples and sample processing at the bench, (ii) rationale and biophysical necessities related to the design and validation of the mass cytometry antibody panel, (iii) the basis for selecting external ligands and ligand concentrations for stimulation of clinical samples, (iv) technical and analytical implications of sample barcoding, (v) the need for mass cytometry data normalization, and (vi) the appropriate use of analytical strategies to relate the large high-dimensional, single-cell dataset to clinical endpoints.

Applying these methodological principles resulted in a high-dimensional assay that allows the quantification of functional attributes of precisely phenotyped immune cell subsets across a range of stimulation conditions. Specifically, the antibody panel was tailored to innate and adaptive immune cells that have been implicated in the pathophysiology of preterm births. Two complementary approaches were implemented to process and analyze the data and maximize knowledge gained from this study. The first approach used manual gating strategies embedded in prior knowledge and statistical analyses that stringently

accounted for multiple comparisons (Bonferroni correction). This approach is best suited to test a specific hypothesis. The second approach implemented a clustering algorithm to agnostically define immune cell subsets based on the expression of all cell-surface markers and infer functional attributes of each cell cluster. This approach produced a large dataset and is hypothesis-generating in nature as it applied a less stringent FDR <1% to detect statistically significant differences. In this study, the second approach generated the hypothesis that LPS-induced TLR4 signaling in classical monocytes separates non-pregnant women with a history of term and preterm birth.

Our results indicated that the distribution of immune cells and the functional attributes (signaling events) of the majority of examined immune cell subsets were similar between the two study groups (Figs. 3 and 5). These results may not be particularly surprising as the studied populations were non-pregnant women. Arguably, differences between women with term and preterm birth may only become apparent, or alternatively, may be more accentuated and detectable during pregnancy. Nevertheless, a study in non-pregnant women is important as it may point to immune traits that exist in the absence of pregnancy.

The unsupervised clustering approach revealed that the prpS6 and pMAPKAPK2 responses to LPS in classical monocyte cell clusters were more pronounced in the preterm than in the term study group (Fig. 6). These results are consistent with the prpS6 and pMAPKAPK2 responses measured in manually-gated classical monocytes (Fig. 5, Supporting Information Table 2), thus reinforcing the biological plausibility of immune features identified using an explorative hierarchical clustering approach. Ligand concentration versus signaling response curves were used to "filter" statistically significant results from the explorative analysis for their biological plausibility. Specifically, only two (prpS6 and pMAPKAPK2 in classical monocytes) out of six statistically significant signaling responses (FDR<1%) occurred in a cell subset that responded to LPS in a ligand-concentration-dependent fashion (Fig. 5). Remarkably, differences between study groups were most apparent at low and "physiological" LPS concentrations (0.1 ng mL^{-1}), suggesting that examining immune cell responses at low concentrations, rather than at maximum and "supra-physiological" concentrations only, may reveal relevant biological information.

The use of mass cytometry dovetails with and expands upon prior efforts that explored distinctive immune features associated with the onset of birth in humans. Previous attempts precluded the detailed characterization of immune cell subsets and the assessment of cell-specific functional attributes (14,36). For example, a study in women at risk for preterm birth, which relied on the bulk analysis of LPS-stimulated responses in PBMCs, did not allow for the differentiation of functional responses among individual cell subsets (14). The lack of single-cell resolution may have undermined the precision of the assay and may explain why a large patient cohort was required to reach statistical significance. In contrast, a power analysis anchored in the present dataset suggests that a follow-up study of pregnant women with a history of preterm or term birth would require a relatively small number of patients. Assuming similar variability in signaling responses, twenty patients per group would provide 90% power to detect a 30% difference in prpS6 or pMAPKAPK2 signaling in classical monocytes (Mann–Whitney test, one-sided, $a = 0.05/6$).

The differences reported are modest. However, the results suggest that in women predisposed to preterm birth, classical monocytes may be prone to mount an exacerbated TLR4 response during the course of pregnancy. Monocytes play a critical role in the maintenance of pregnancy as precursors to decidual macrophages, which represent over 20% of the human decidual leukocyte population (24). While these innate cells are prime candidates for participation in placental tissue remodeling, serving as pathogen sensors and effector immune cells in inflammatory mechanisms of preterm birth, their role in the maintenance of human pregnancy is poorly understood. Our data, however, are consistent with studies in mouse models of preterm birth, which suggest that TLR4 signaling in monocytes and macrophages is an important immune mechanism that controls the onset of birth (25,37).

This study has certain limitations. There was significant variability in the gestational age at delivery of women with a history of preterm birth (range 24–34 weeks). The reported differences might have been accentuated if stricter inclusion criteria had been selected for extremes of gestational age or patients with a history of repeat preterm birth only. By design, the study focused on immune responses to LPS stimulation, restricting the analysis to LPS-responsive immune cell types. Future studies are underway to expand the analysis to functional responses in other cell types (including NK cells, B cells, and T-cell subsets).

The implementation of mass cytometry in clinical studies is of significant interest. This report highlights important issues to consider when obtaining and analyzing high-quality mass cytometry data. Our results set the stage for longitudinal studies tracking pregnancy-induced changes in the peripheral immune system of women with a history of preterm or term birth, as well as women who will go on to deliver term or pre-term. These studies will also capitalize on the newly generated hypothesis focusing on the role of TLR4 signaling in monocyte subsets, and shed light on important innate mechanisms that control maintenance of pregnancy in humans.

Supplementary Material

Refer to Web version on PubMed Central for supplementary material.

Acknowledgments

Literature Cited

1. Bendall SC, Simonds EF, Qiu P, Amir el AD, Krutzik PO, Finck R, Bruggner RV, Melamed R, Trejo A, Ornatsky OI, Balderas RS, Plevritis SK, Sachs K, Pe'er D, Tanner SD, Nolan GP. Single-cell mass cytometry of differential immune and drug responses across a human hematopoietic continuum. Science. 2011; 332:687–696. [PubMed: 21551058]

2. Bjornson ZB, Nolan GP, Fantl WJ. Single-cell mass cytometry for analysis of immune system functional states. Curr Opin Immunol. 2013; 25:484–494. [PubMed: 23999316]

3. Bendall SC, Nolan GP. From single cells to deep phenotypes in cancer. Nat Biotechnol. 2012; 30:639–647. [PubMed: 22781693]

4. Gaudilliere B, Fragiadakis GK, Bruggner RV, Nicolau M, Finck R, Tingle M, Silva J, Ganio EA, Yeh CG, Maloney WJ, Huddleston JI, Goodman SB, Davis MM, Bendall SC, Fantl WJ, Angst MS, Nolan GP. Clinical recovery from surgery correlates with single-cell immune signatures. Sci Transl Med. 2014; 6:255ra131.

5. Tarnok A. Revisiting the crystal ball–high content single cells analysis as predictor of recovery. Cytometry A. 2015; 87A:97–98. [PubMed: 25614362]

6. Leipold MD. Another step on the path to mass cytometry standardization. Cytometry A J Int Soc Anal Cytol. 2015; 87:380–382.

7. Yao Y, Liu R, Shin MS, Trentalange M, Allore H, Nassar A, Kang I, Pober JS, Montgomery RR. CyTOF supports efficient detection of immune cell subsets from small samples. J Immunol Methods. 2014; 415:1–5. [PubMed: 25450003]

8. Finck R, Simonds EF, Jager A, Krishnaswamy S, Sachs K, Fantl W, Pe'er D, Nolan GP, Bendall SC. Normalization of mass cytometry data with bead standards. Cytometry A. 2013; 83A:483–494. [PubMed: 23512433]

9. Leipold MD, Maecker HT. Mass cytometry: Protocol for daily tuning and running cell samples on a CyTOF mass cytometer. J Vis Exp. 2012:e439869.

10. Goldenberg RL, Culhane JF, Iams JD, Romero R. Epidemiology and causes of pre-term birth. Lancet. 2008; 371:75–84. [PubMed: 18177778]

11. Liu L, Oza S, Hogan D, Perin J, Rudan I, Lawn JE, Cousens S, Mathers C, Black RE. Global, regional, and national causes of child mortality in 2000–13, with projections to inform post-2015 priorities: An updated systematic analysis. Lancet. 2015; 385:430–440. [PubMed: 25280870]

12. Romero R, Dey SK, Fisher SJ. Preterm labor: One syndrome, many causes. Science. 2014; 345:760–765. [PubMed: 25124429]

13. Zhao H, Kalish F, Schulz S, Yang Y, Wong RJ, Stevenson DK. Unique roles of infiltrating myeloid cells in the murine uterus during early to midpregnancy. J Immunol. 2015; 194:3713–3722. [PubMed: 25780045]

14. Harper M, Li L, Zhao Y, Klebanoff MA, Thorp JM Jr, Sorokin Y, Varner MW, Wapner RJ, Caritis SN, Iams JD, Carpenter MW, Peaceman AM, Mercer BM, Sciscione A, Rouse DJ, Ramin SM, Anderson GD. Eunice Kennedy Shriver National Institute of Child H and Human Development Maternal-Fetal Medicine Units, N. Change in mononuclear leukocyte responsiveness in

midpregnancy and subsequent preterm birth. Obstet Gynecol. 2013; 121:805–811. [PubMed: 23635681]

15. Macey MG, McCarthy DA, Vordermeier S, Newland AC, Brown KA. Effects of cell purification methods on CD11b and L-selectin expression as well as the adherence and activation of leucocytes. J Immunol Methods. 1995; 181:211–219. [PubMed: 7538158]

16. Souques F, Duperray C, Pene J, Bousquet J, Arnoux B. Modification of surface marker expression on CD14 monocytes of allergic patients after lysis or Ficoll purification. J Immunol Methods. 1997; 204:153–160. [PubMed: 9212832]

17. Lundahl J, Hallden G, Hallgren M, Skold CM, Hed J. Altered expression of CD11b/CD18 and CD62L on human monocytes after cell preparation procedures. J Immunol Methods. 1995; 180:93–100. [PubMed: 7534806]

18. Baechler EC, Batliwalla FM, Karypis G, Gaffney PM, Moser K, Ortmann WA, Espe KJ, Balasubramanian S, Hughes KM, Chan JP, Begovich A, Chang SY, Gregersen PK, Behrens TW. Expression levels for many genes in human peripheral blood cells are highly sensitive to ex vivo incubation. Genes Immun. 2004; 5:347–353. [PubMed: 15175644]

19. Appay V, Reynard S, Voelter V, Romero P, Speiser DE, Leyvraz S. Immuno-monitoring of CD8+ T cells in whole blood versus PBMC samples. J Immunol Methods. 2006; 309:192–199. [PubMed: 16403411]

20. Lu Y, Ahmed S, Harari F, Vahter M. Impact of Ficoll density gradient centrifugation on major and trace element concentrations in erythrocytes and blood plasma. J Trace Elements Med Biol Organ Soc Miner Trace Elements. 2015; 29:249–254.

21. Schulz, KR.; Danna, EA.; Krutzik, PO.; Nolan, GP. Single-cell phospho-protein analysis by flow cytometry. In: Coligan, John E., et al., editors. Curr Protocols Immunol. Vol. 17. 2012. p. 11-20.

22. Kay AW, Fukuyama J, Aziz N, Dekker CL, Mackey S, Swan GE, Davis MM, Holmes S, Blish CA. Enhanced natural killer-cell and T-cell responses to influenza A virus during pregnancy. Proc Natl Acad Sci USA. 2014; 111:14506–14511. [PubMed: 25246558]

23. Bastek JA, Gomez LM, Elovitz MA. The role of inflammation and infection in pre-term birth. Clin Perinatol. 2011; 38:385–406. [PubMed: 21890015]

24. Erlebacher A. Immunology of the maternal-fetal interface. Annu Rev Immunol. 2013; 31:387–411. [PubMed: 23298207]

25. Elovitz MA, Wang Z, Chien EK, Rychlik DF, Phillippe M. A new model for inflammation-induced preterm birth: The role of platelet-activating factor and Toll-like receptor-4. Am J Pathol. 2003; 163:2103–2111. [PubMed: 14578208]

26. Tricot S, Meyrand M, Sammicheli C, Elhmouzi-Younes J, Corneau A, Bertholet S, Malissen M, Le Grand R, Nuti S, Luche H, Cosma A. Evaluating the efficiency of isotope transmission for improved panel design and a comparison of the detection sensitivities of mass cytometer instruments. Cytometry A. 2015; 87A:357–368. [PubMed: 25704858]

27. Kraus TA, Sperling RS, Engel SM, Lo Y, Kellerman L, Singh T, Loubeau M, Ge Y, Garrido JL, Rodriguez-Garcia M, Moran TM. Peripheral blood cytokine profiling during pregnancy and post-partum periods. Am J Reprod Immunol. 2010; 64:411–426. [PubMed: 20712812]

28. Bodenmiller B, Zunder ER, Finck R, Chen TJ, Savig ES, Bruggner RV, Simonds EF, Bendall SC, Sachs K, Krutzik PO, Nolan GP. Multiplexed mass cytometry profiling of cellular states perturbed by small-molecule regulators. Nat Biotechnol. 2012; 30:858–867. [PubMed: 22902532]

29. Zunder ER, Finck R, Behbehani GK, Amir el AD, Krishnaswamy S, Gonzalez VD, Lorang CG, Bjornson Z, Spitzer MH, Bodenmiller B, Fantl WJ, Pe'er D, Nolan GP. Palladium-based mass tag cell barcoding with a doublet-filtering scheme and single-cell deconvolution algorithm. Nat Protocols. 2015; 10:316–333. [PubMed: 25612231]

30. Maecker HT, McCoy JP, Nussenblatt R. Standardizing immunophenotyping for the human immunology project. Nat Rev Immunol. 2012; 12:191–200. [PubMed: 22343568]

31. Beutler B. Inferences, questions and possibilities in Toll-like receptor signalling. Nature. 2004; 430:257–263. [PubMed: 15241424]

32. Bruggner RV, Bodenmiller B, Dill DL, Tibshirani RJ, Nolan GP. Automated identification of stratifying signatures in cellular subpopulations. Proc Natl Acad Sci USA. 2014; 111:E2770–E2777. [PubMed: 24979804]

33. Aghaeepour N, Finak G, Flow CAPC, Hoos H, Mosmann TR, Brinkman R, Gottardo R, Scheuermann RH. Consortium D. Critical assessment of automated flow cytometry data analysis techniques. Nat Methods. 2013; 10:228–238. [PubMed: 23396282]

34. Tusher VG, Tibshirani R, Chu G. Significance analysis of microarrays applied to the ionizing radiation response. Proc Natl AcadSci USA. 2001; 98:5116–5121.

35. Tibshirani R, Hastie T, Narasimhan B, Chu G. Diagnosis of multiple cancer types by shrunken centroids of gene expression. Proc Natl Acad Sci USA. 2002; 99:6567–6572. [PubMed: 12011421]

36. Bardou M, Hadi T, Mace G, Pesant M, Debermont J, Barrichon M, Wendremaire M, Laurent N, Sagot P, Lirussi F. Systemic increase in human maternal circulating CD14+CD16– MCP-1+ monocytes as a marker of labor. Am J Obstet Gynecol. 2014; 210:70, e71–e79. [PubMed: 23994222]

37. Gonzalez JM, Franzke CW, Yang F, Romero R, Girardi G. Complement activation triggers metalloproteinases release inducing cervical remodeling and preterm birth in mice. Am J Pathol. 2011; 179:838–849. [PubMed: 21801872]
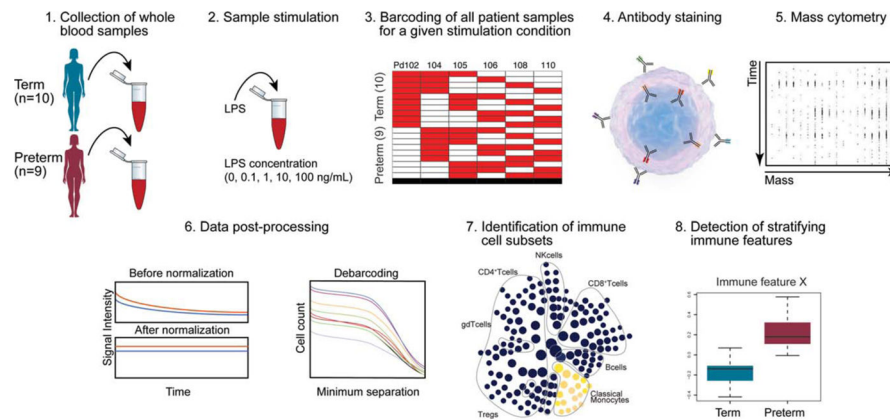
Figure 1. Study design and experimental workflow

Whole blood samples were collected from non-pregnant women with a history of term (n = 10) or preterm (n = 9) birth (Panel 1). Within 30 min of venipuncture, separate whole blood aliquots were stimulated *ex vivo* with different concentrations of LPS (0, 0.1, 1, 10, and 100 ng mL^{-1}), fixed, and frozen at −80°C (Panel 2). For each LPS concentration, all samples were barcoded using a combination of three palladium (Pd) mass tags, pooled, and processed simultaneously (Panel 3). Pooled samples were stained using a combination of 27 cell-surface markers and 11 functional markers (Panel 4) and analyzed by mass cytometry (Panel 5). The resulting dataset was normalized to account for changes in machine sensitivity and then de-barcoded (Panel 6). Unsupervised hierarchical clustering and manual gating strategies were applied to visualize and quantify patient-specific signaling responses in immune cell subsets spanning the entire immune system. Shown is a visual representation of a cluster hierarchy plot (Panel 7). Contoured are clusters that fall within canonical immune cell subsets. Immune features (cell frequency or signaling responses) that differed significantly between the term and preterm study groups were identified using two complementary statistical approaches (Panel 8).
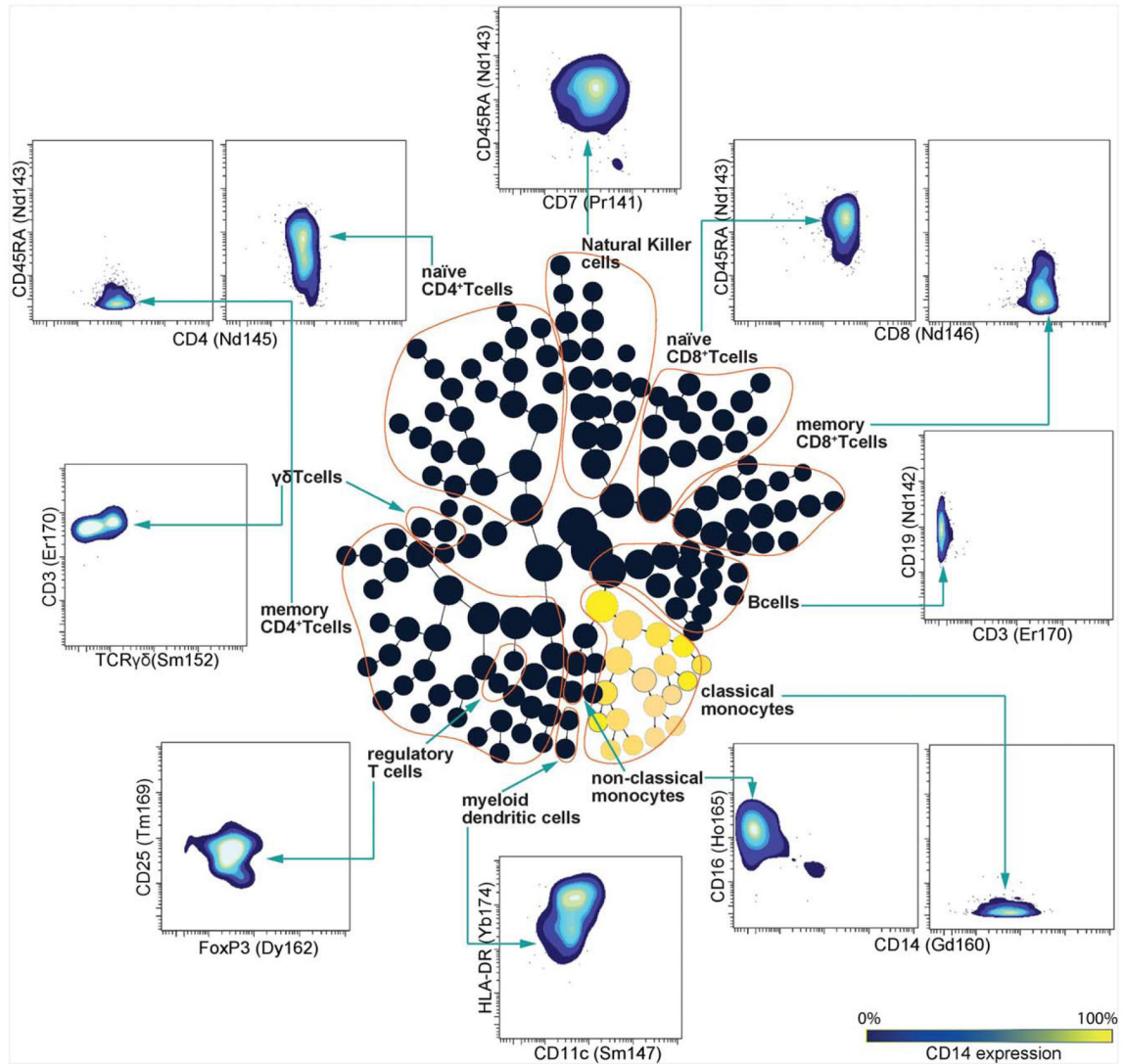
Figure 2.
Strategies for immune cell phenotyping of patient samples. Two complementary approaches were used to identify immune cell subsets. The first approach (Supporting Information Fig. 1) used the expression level of a limited number of canonical cell-surface markers anchored in prior knowledge to manually gate 12 immune cell subsets. The second approach identified cell clusters with distinct cell-surface signatures based on the expression of all phenotypic markers using an unsupervised clustering algorithm (32). To avoid biasing the clustering toward the CD66$^+$ granulocyte population, which represented over 40% of the total immune cells, the clustering analysis included CD45$^+$CD66$^-$ cells only. The clustering hierarchy is visually represented by the graph in the center. Coloring the CITRUS clustering tree by surface marker expression (in this example CD14) identifies cell clusters that represent canonical immune cell subsets (classical monocyte are highlighted in yellow). Blue arrows indicate biaxial density plots of groups of cell clusters contained within canonical immune cell subsets (contoured by red circles).
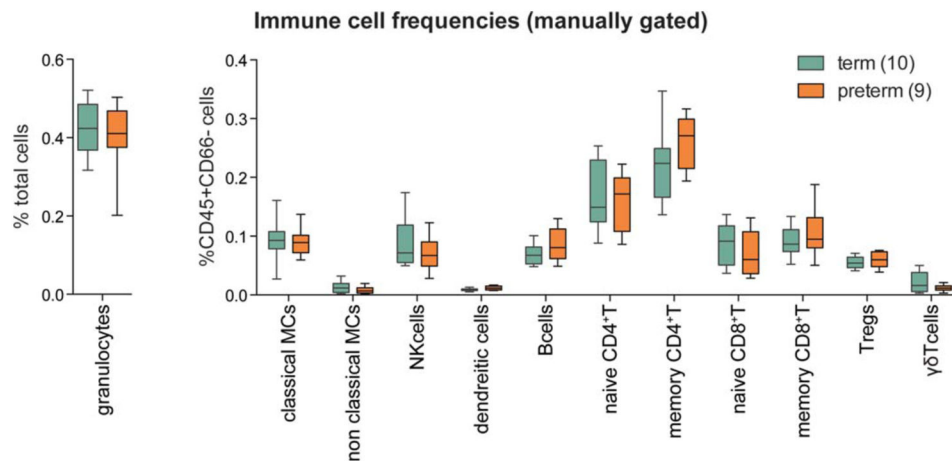
Figure 3.
Immune cell distributions in patient samples from the term and preterm study groups. Frequencies of granulocytes (left panel), classical monocytes (cMCs), non-classical monocytes (ncMCs), myeloid dendritic cells (DCs), natural killer (NK) cells, B cells, naive and memory CD4$^+$ T cells, and naive and memory CD8$^+$ T cells, regulatory T cells (T_{regs}), and $\gamma\delta$T cells are depicted for 10 patients with a history of term birth (teal) and 9 patients with a history of preterm birth (orange). Granulocyte frequency was quantified as percent of total hematopoietic cells (CD61$^-$CD235$^-$). All other cell frequencies are expressed as percent total of mononuclear cells (CD45$^+$CD66$^-$). Results are shown as box plots (median and interquartile range) and whiskers (range). Immune cell frequencies did not differ between the two study groups (Bonferroni adjusted *P* value >0.004).
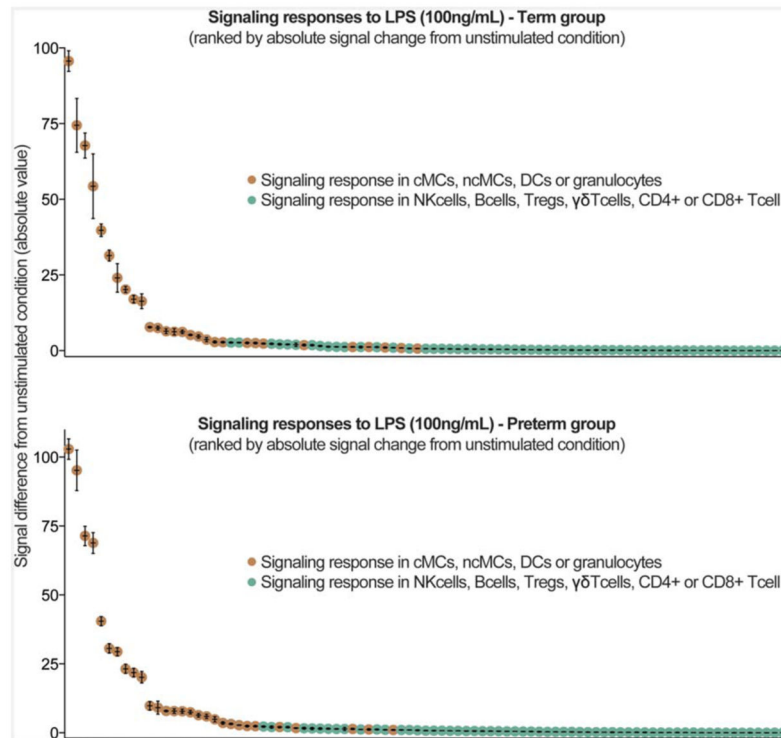
Figure 4.
Signaling responses to maximum LPS stimulation (100 ng mL^{-1}) across immune cell subsets. Depicted in rank-order are the signal intensity changes (absolute difference in signal intensity or raw counts between the baseline condition and the response to 100 ng mL^{-1} LPS) of the seven functional markers pP38, pERK1/2, pMAPKAPK2, prpS6, pCREB, pNFκB, and IκB as assessed in 12 manually gated cell types (Fig. 2). Results are separately shown for patients with a history of term (upper panel) and preterm birth (lower panel). Signaling responses in monocytes, dendritic cells (DCs), and granulocytes (orange circles) were robust (median differences 7.6 [IQR: 3.4–43.4] in the term group, and 7.9 [IQR 3.1–33.1] in the preterm group), while signaling responses in natural killer (NK) cells, B cells, CD4$^+$ and CD8$^+$ T cells (naive and memory), regulatory T cells (T_{regs}), and $\gamma\delta$Tcells (teal circles) were minimal or absent (median differences 0.33 [IQR: 0.07–1.0] in the term group and 0.37 [IQR: 0.1–0.96] in the preterm group). Results are represented as ranked mean difference (absolute values) ± SEM.
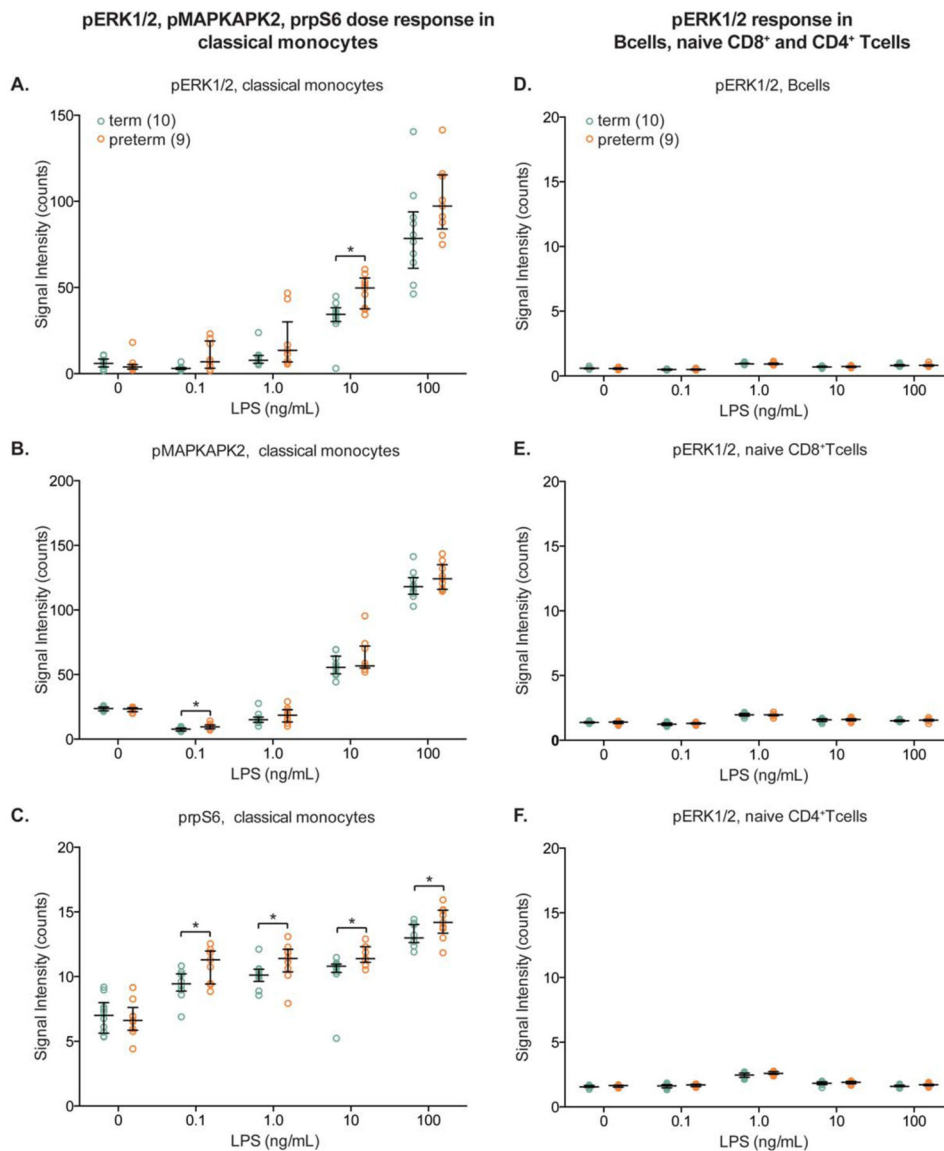
Figure 5. Dose-dependent and cell-type-specific signaling responses to LPS in patient samples from the term and preterm study groups

Signal intensities (raw counts) were quantified for seven functional markers (pERK1/2, pMAPKAPK2, prpS6, pP38, pCREB, pNFκB, and IκB) in 12 manually gated cell types (Fig. 2) in response to increasing LPS concentrations (0, 0.1, 1, 10, 100 ng mL^{-1}) for patient samples from the term (teal circles) and the preterm (orange circles) study groups. **A–G**. Dose-response curves are shown for classical monocytes. Results are shown as median signal intensity and interquartile range (* indicates a *P* value <0.05).
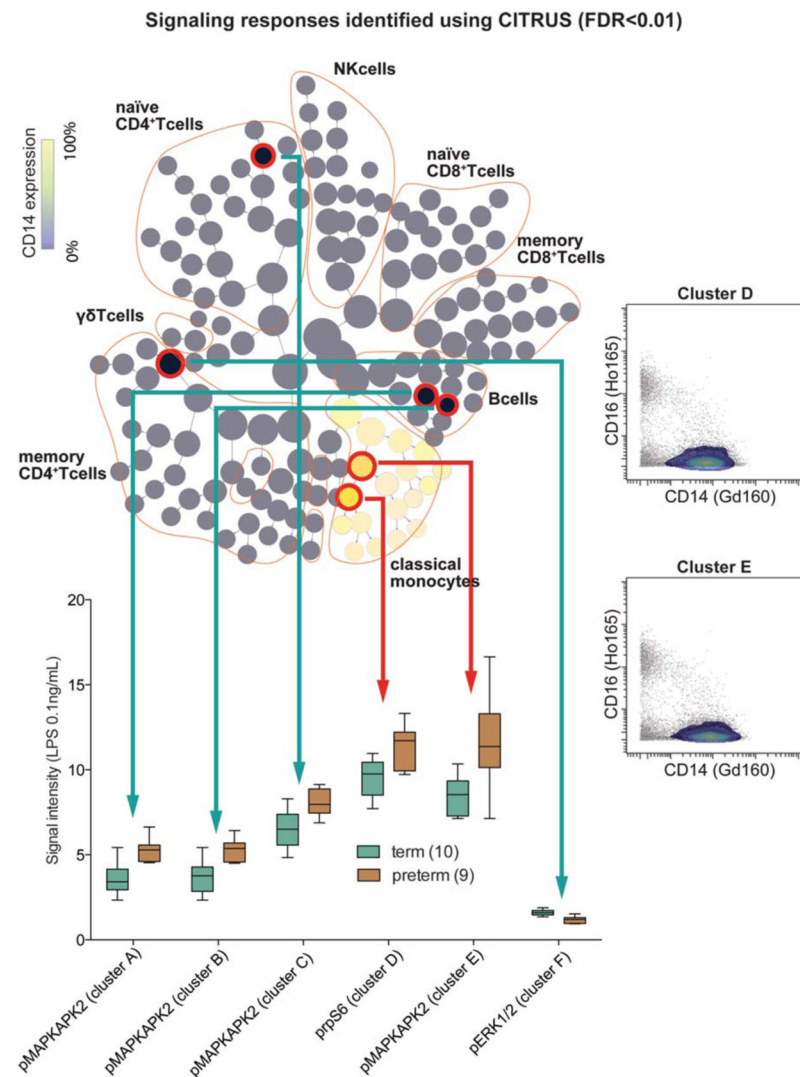
Figure 6.
rpS6 and MAPKAPK2 responses to low-dose LPS in classical monocytes is more pronounced in women with a history of pre-term birth. Shown is a representation of an unsupervised clustering hierarchy. Cell clusters for which signaling responses were statistically different between study groups (FDR <0.01, SAM) are highlighted by red circles. Arrows originating from these circles point to the respective signaling response to 0.1 ng mL^{-1} LPS. Blue arrows indicate that the signaling response in the particular cell cluster did not follow a ligand concentration-dependent activation pattern and, therefore, may be less plausible from a biological perspective. Red arrows indicate that the signaling response in the particular cell cluster did follow a ligand concentration-dependent activation pattern. Results are shown as box plots (median signal intensity and interquartile range) and whiskers (min to max signal intensity). Shown on the right are biaxial plots of CD14$^+$CD16$^-$ cells contained in clusters **D** and **E** (blue contour) overlaid on a dot plot of all

CD33$^+$CD3$^-$CD7$^-$CD66$^-$ monocytes of a representative patient sample. Overlaid biaxial plots for clusters **A**, **B**, **C**, **F** are shown in Supporting Information Figure 2.